Journal of Hazardous Materials 161 (2009) 231–240

Contents lists available at ScienceDirect

Journal of Hazardous Materials

journal homepage: www.elsevier.com/locate/jhazmat

Study the adsorption of phenol from aqueous solution on hydroxyapatite nanopowders

Kaili Lin[a,b,*], Jiayong Pan[a], Yiwei Chen[a], Rongming Cheng[a,*], Xuecheng Xu[a]

[a] Center of Functional Nanomaterials and Devices, Engineering Research Center for Anophotonics & Advanced Instrument Ministry of Education, East China Normal University, 3663 North Zhongshan Road, Shanghai 200062, PR China
[b] Shanghai Institute of Ceramics, Chinese Academy of Sciences, 1295 Dingxi Road, Shanghai 200050, PR China

ARTICLE INFO

Article history:
Received 6 August 2007
Received in revised form 17 March 2008
Accepted 19 March 2008
Available online 22 March 2008

Keywords:
Phenol adsorption
Hydroxyapatite nanopowders
Equilibrium
Kinetic
Thermodynamic

ABSTRACT

In this study, the hydroxyapatite (HAp) nanopowders prepared by chemical precipitation method were used as the adsorbent, and the potential of HAp nanopowders for phenol adsorption from aqueous solution was studied. The effect of contact time, initial phenol concentration, pH, adsorbent dosage, solution temperature and adsorbent calcining temperature on the phenol adsorption, and the adsorption kinetic, equilibrium and thermodynamic parameters were investigated. The results showed that the HAp nanopowders possessed good adsorption ability to phenol. The adsorption process was fast, and it reached equilibrium in 2 h of contact. The initial phenol concentration, pH and the adsorbent calcining temperature played obvious effects on the phenol adsorption capacity onto HAp nanopowders. Increase in the initial phenol concentration could effectively increase the phenol adsorption capacity. At the same time, increase in the pH to high-acidity or to high-alkalinity also resulted in the increase in the phenol adsorption capacity. Increase in the HAp dosage could effectively increase the phenol adsorption percent. However, the higher calcining temperature of HAp nanopowders could obviously decrease the adsorption capacity. The maximum phenol adsorption capacity was obtained as 10.33 mg/g for 400 mg/L initial phenol concentrations at pH 6.4 and 60 °C. The adsorption kinetic and the isotherm studies showed that the pseudo-second-order model and the Freundlich isotherm were the best choices to describe the adsorption behaviors. The thermodynamic parameters suggested that the adsorption of phenol onto HAp was physisorption, spontaneous and endothermic in nature.

1. Introduction

The pollutants of phenol (shown in Fig. 1) and related compounds are widely produced by the coal conversion, petroleum refining, resin and plastic industries, etc. [1]. These compounds are toxic to humans and aquatic lives, causing oxygen demand in receiving waters [2,3]. Their presence in water supplies is noticed as a bad taste and odor. Therefore, the wastewaters containing phenolic compounds must be treated before their discharge into the water streams [4].

Conventional methods for the removal of phenolic pollutants in aqueous solutions can be divided into three main categories: physical, chemical and biological treatment [5]. Among them, physical adsorption method is generally considered to be the best, effective, low-cost and most frequently used method for the removal of phenolic pollutants. The most popular and widely used adsorbent material is activated carbon [6–8]. However, the high initial cost and the need for a costly regeneration system make the activated carbon less economically viable as excellent adsorbent [9–12]. Therefore, the search for low cost and easily available adsorbents has led many researchers to search more economic and efficient techniques of using the natural and synthetic materials as adsorbents [3,12–19]. Recently, using the natural and synthetic inorganic materials as adsorbents has become one hot research field [3,13–19]. A significant aspect of the inorganic adsorbents is that the bonding forces between the adsorbent and the adsorbate are usually weaker than those encountered in activated carbon or polymer adsorbents. On the other hand, the inorganic adsorbents also possess excellent thermal stability. Therefore, the regeneration of the inorganic adsorbents can be accomplished by simple and non-destructive methods, such as solvent washing or calcining, which provides the potential approaches to recover these adsorbents. However, the

* Corresponding authors at: Center of Functional Nanomaterials and Devices, Engineering Research Center for Anophotonics & Advanced Instrument Ministry of Education, East China Normal University, 3663 North Zhongshan Road, Shanghai 200062, PR China. Tel.: +86 21 52412810; fax: +86 21 52413903.
E-mail addresses: lklecnu@yahoo.com.cn (K. Lin), rmcheng@phy.ecnu.edu.cn (R. Cheng).

0304-3894/$ – see front matter © 2008 Elsevier B.V. All rights reserved.
doi:10.1016/j.jhazmat.2008.03.076

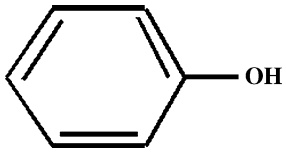

Fig. 1. The chemical structure of phenol molecule.

adsorption ability of the traditional inorganic adsorbent materials is low due to their low surface area. It is well known that the nano-size adsorbents possess excellent surface properties, such as large accessible internal and/or external surface. Therefore, the nano-size adsorbents possess high adsorption ability. In these regards, the nano-size inorganic material is one of the most widely used candidates for adsorbents to remove the pollutants from aqueous solutions.

Hydroxyapatite (HAp) nanopowders possess high biocompatibility and adsorption properties, and have been widely used as carriers for drugs and genes, adsorbents for chromatography to separate proteins, and removal of heavy metal ions to recover the contaminated soils, wastewater and fly ashes, etc. [20–25]. However, as to our knowledge, the adsorption and removal of the phenolic compounds by HAp has not been reported.

The objective of this study was to investigate the potential candidate of HAp nanopowders as a new biocompatible adsorbent for the adsorption of phenol pollutants from aqueous solutions. The effect of contact time, initial phenol concentration, pH, adsorbent dosage, solution temperature and adsorbent calcining temperature on the phenol adsorption, and the adsorption kinetic, equilibrium and thermodynamic parameters at various temperatures and concentrations were investigated.

2. Materials and methods

2.1. Adsorbent

The hydroxyapatite (HAp) nanopowders were synthesized by chemical precipitation method. The procedure employed for the synthesis of HAp nanopowders is as follows and all reagents were analytical grade, purchased from Shanghai Chemical Co., Ltd., PR China and used without further purification. First, 0.5 M $Ca(NO_3)_2$ solutions and 0.3 M $(NH_4)_2HPO_4$ solutions were obtained by dissolving $Ca(NO_3)_2{\cdot}4H_2O$ and $(NH_4)_2HPO_4$ in distilled water, respectively, and the pH of both solutions was adjusted to 11.0 by adding ammonia solution. The reactant molar ratio of Ca/P was kept at 1.667. The solution of $(NH_4)_2HPO_4$ was dropwisely added into the $Ca(NO_3)_2$ solution, and the white suspension was obtained. During the addition, the pH of the suspension was maintained at 11.0 using ammonia solution. After the complete addition, the suspension was further stirred for 24 h. Then the obtained suspension was filtrated and washed with distilled water and anhydrous ethanol for three times. The resultant powders were dried at 100 °C for 24 h, and then calcined at 120, 600 and 900 °C for 2 h, respectively. The final products calcined at different temperatures were used as the adsorbents for the phenol.

2.2. Adsorbent characterization

The synthesized powders were characterized by X-ray diffraction (XRD: D/max 2550V, Rigaku, Japan) with mono-chromated Cu Kα radiation. The morphology and size of the synthesized powders were characterized by field emission transmission electron microscopy (FETEM: JEM-2100F, JEOL, Japan). The chemical composition of the synthesized powders was analysed by inductively coupled plasma atomic emission spectroscopy (ICP-AES; VISTA AX, Varian Co., USA). The specific surface area of HAp nanopowders calcined at different temperatures was determined by nitrogen adsorption at 77 K (Micromeritics ASAP 2010, USA). Surface areas were calculated from adsorption data using BET equation.

2.3. Phenol solutions

Phenol used in this study were obtained from Shanghai Chemical Co., Ltd. (analytical grade) and used without further purification. Stock solutions were prepared by weighing out the pure crystalline solid in distilled water for phenol. All solutions used in this study were diluted with distilled water as required. The initial concentrations of phenol tested were 2, 6, 10, 20, 30, 100, 200, 300 and 400 mg/L. The prepared phenol solutions were stored in brown color glass reservoirs to prevent photo-oxidation. The initial pH of the working solution was adjusted by addition of 0.1 mol/L HCl or 0.01 mol/L NaOH solution.

2.4. Methods of adsorption studies

Batch adsorption studies were conducted by shaking the flasks for a period of time using an air bath mechanical shaker. The experimental process was as followings: put a certain quantity of HAp nanopowders into conical flasks, then, added the phenol solution in single component system, vibrated sometime at a constant speed of 240 rpm in a shaking air bath. After a period of shaking and contact time, took out the conical flasks, filtrated to separate HAp nanopowders and the solution. The phenol concentration analysis of filtrate solution was immediately measured with UV/vis spectrophotometer (UV-2802S, Shanghai Unico Co., Ltd., PR China) at a 269 nm wavelength [26]. The phenol adsorption capacity (q_e, mg/g) was determined as follows:

$$q_e = (C_0 - C_t)\frac{V}{m} \quad (1)$$

where C_0 is the initial phenol concentration (mg/L), C_t is the phenol concentration at time t (mg/L), V is the volume (L) of aqueous solution containing phenol, and m is the mass of HAp adsorbent (g). The calibration plot of absorbance versus concentration for phenol showed a linear variation up to 40 mg/L concentrations. Therefore, the samples with higher phenol concentration (>40 mg/L) were diluted with distilled water, whenever necessary, to make the concentration less than 40 mg/L, for the accurate determination of phenol concentration with the help of the linear portion of the cal-

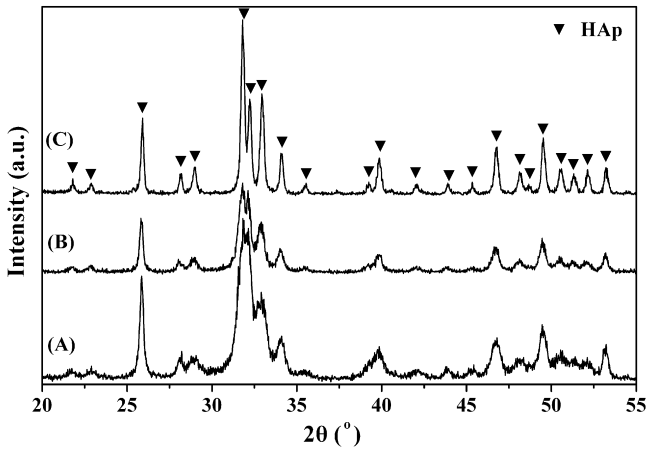

Fig. 2. XRD pattern of the synthesized HAp nanopowders calcined at 120 °C (A), 600 °C (B) and 900 °C (C).

ibration curve. In order to evaluate the statistical significance of data in the adsorption experiments, a preliminary experiment was also repeated under identical conditions, showing that the error reproducibility of the measurements was within 5% in the adsorption experiments.

The adsorption of the phenol was calculated by the difference in their initial and final concentrations. Effect of pH (2–11), contact time (0.25–8 h), adsorbent dosage (2–12 g/L), temperature (20, 40 and 60 °C) and adsorbent calcining temperature (120, 600 and 900 °C) on the phenol adsorption was studied. Each experiment was repeated three times and the given results were the average values.

2.5. Batch kinetic, equilibrium and thermodynamic studies

To investigate the kinetics, equilibrium and thermodynamic of the phenol adsorption on HAp nanopowders, 25 mg HAp nanopowders was added into a conical flask containing 25 mL phenol solution with pH of 6.4 at various concentrations, and then vibrated at a constant speed of 240 rpm using an air bath mechanical shaker. In order to study the adsorption isotherms and thermodynamic, 4 h of contact were applied to allow attainment of equilibrium at a constant temperature of 20, 40 and 60 °C, respectively. For the kinetic study, the samples were contacted for time intervals at various temperatures. After shaking and contacting, took out the conical flasks, filtrated to separate HAp nanopowders and the solution. The phenol concentration of the filtrate solution was immediately measured. The phenol adsorption capacity (q_e, mg/g) was calculated according to Eq. (1). In the present study, the pseudo-first-order [27], pseudo-second-order [28] and intraparticle diffusion model [29] were used to characterize the kinetic models. The Langmuir [30] and Freundlich [31] models were used to describe the equilibrium nature of phenol adsorption onto HAp nanopowders. The

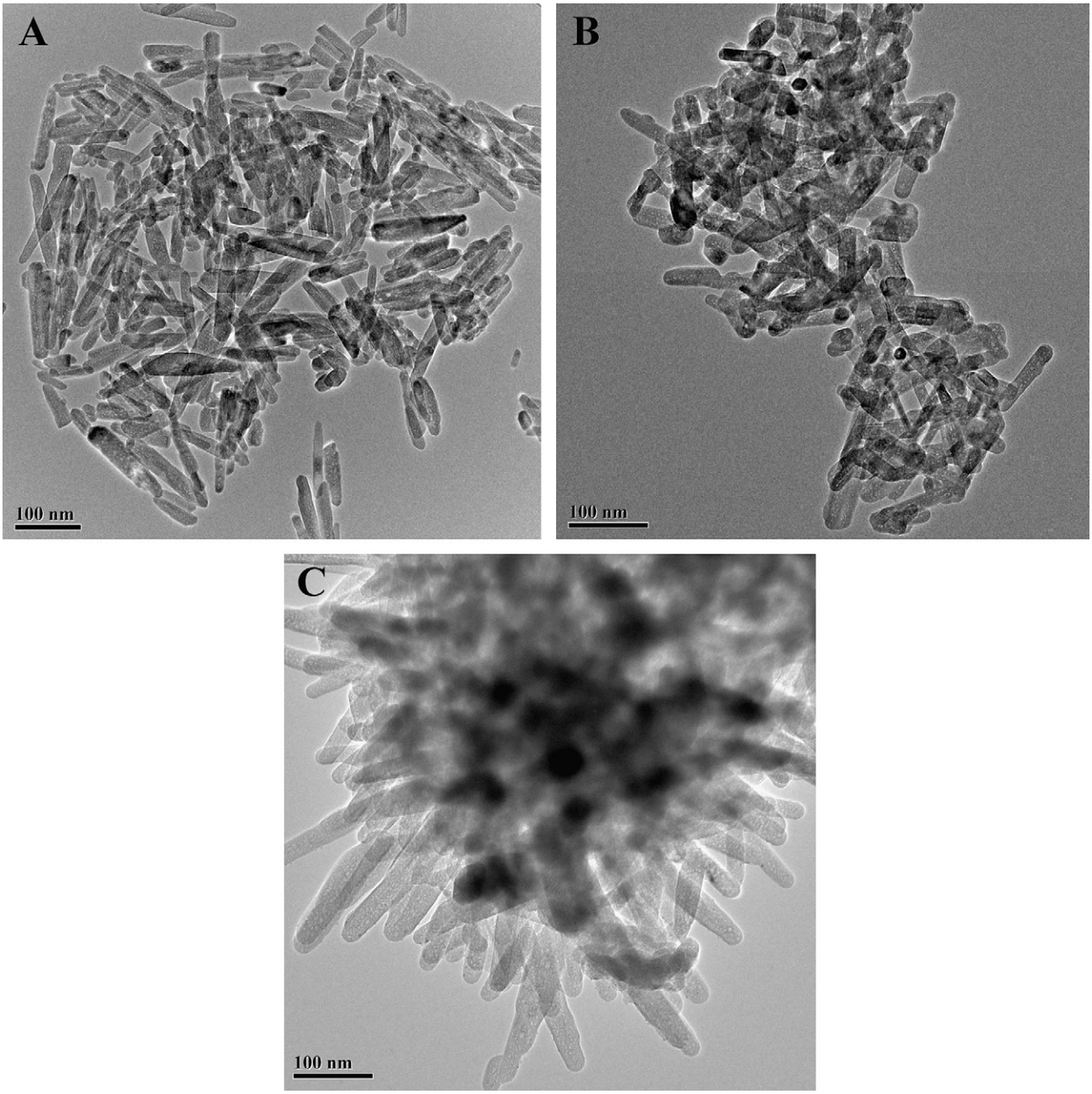

Fig. 3. FETEM image of the synthesized HAp nanopowders calcined at 120 °C (A), 600 °C (B) and 900 °C (C).

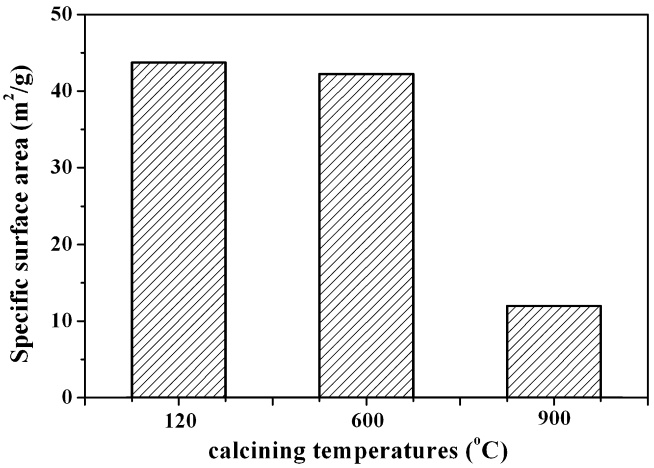

Fig. 4. Effect of calcining temperatures on the specific surface area of the synthesized HAp nanopowders.

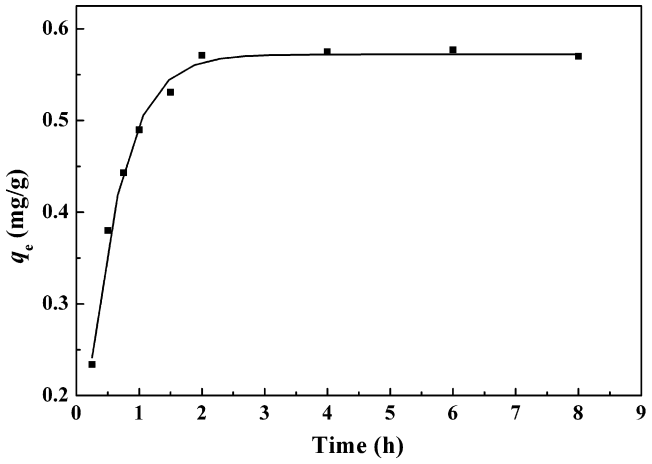

Fig. 5. Effect of contact time on phenol adsorption by HAp nanopowders at given conditions: C_0 = 10 mg/L, pH 6.4, dosage = 4 g/L at 20 °C, and adsorbents calcined at 120 °C.

equilibrium constants were used to calculate the thermodynamic parameters, such as the change of Gibbs free energy (ΔG°), enthalpy (ΔH°) and entropy (ΔS°).

3. Results and discussion

3.1. Characterization of the HAp nanopowders

Fig. 2 shows the XRD patterns of the synthesized powders calcined at the different temperatures for 2 h. All the samples were identified as HAp (JCPDS card: No. 24-0033). It could be seen that there were numerous sharp peaks and low background in the XRD pattern of the HAp powders. Meanwhile, the XRD pattern of the samples did not reveal any other phases than HAp. It is clear to see that increase the calcining temperature result in the higher crystalinity. The shape of the sharp diffraction peaks also indicates that the synthesized samples are well crystallized.

The FETEM image (Fig. 3) indicated that the synthesized HAp powders calcined at different temperatures were needle-like shape, 20–30 nm in diameter and 30–120 nm in length with aspect ratio ranging from 3 to 6. The results also showed that increased the calcining temperatures resulted in the higher aggregation. The aggregation will decrease the specific surface area (SSA), which may ultimately decrease the adsorption capacity of phenol on HAp nanopowders.

Fig. 4 shows the effect of calcining temperatures on the SSA of HAp nanopowders. It is clear to see that the SSA decreased with the increase in the calcining temperature. The HAp nanopowders calcined at 120, 600 and 900 °C had a SSA of 43.75, 42.26 and 11.98 m^2/g, respectively. The decrease of the SSA was attributed to the aggregation of the powders after calcining at high temperature. All the powders calcined at different temperatures have the similar Ca/P molar ration of 1.665, which was close to the theoretical value of 1.667.

3.2. Effect of contact time on phenol adsorption

The adsorption rate of organic pollutants by the adsorbents is relatively rapid and the adsorption equilibrium can reach in less than 24 h [17,32]. Fig. 5 shows the effect of contact time on the adsorption of the phenol on HAp nanopowders. The adsorption equilibrium of phenol was achieved after 2 h and no remarkable changes were observed for longer contact time, which also indicated that the adsorption rate of phenol on HAp nanopowders was much faster than that of some other normal adsorbents for phenol [17,32]. The rapid adsorption of phenol on HAp nanopowders ensures that sufficient time is available for adsorption equilibration to get at the usual operator condition of the adsorption. However, for subsequent experiments, the samples were left for 4 h to ensure the adsorption equilibrium. The equilibrium time of different initial phenol concentrations was also conducted and the results showed that the initial phenol concentrations had little effect on the adsorption equilibrium time.

3.3. Effect of pH on phenol adsorption

It is well known that the most critical parameter affecting the adsorption process in the removal of phenol by the adsorption method is the pH of the adsorption medium. This is due to the charge of the adsorbate and the adsorbent often depending on the pH of the solution. The adsorption of phenol on HAp nanopowders was studied at different initial pH between 2 and 11. The pH before and after adsorption was also measured and the results showed that the difference between the two measured values of pH was less than 0.2. Fig. 6 shows the effect of the initial solution pH on the phenol adsorption onto HAp nanopowders at the given conditions. It is clear to see that the adsorption capacity decreases with increas-

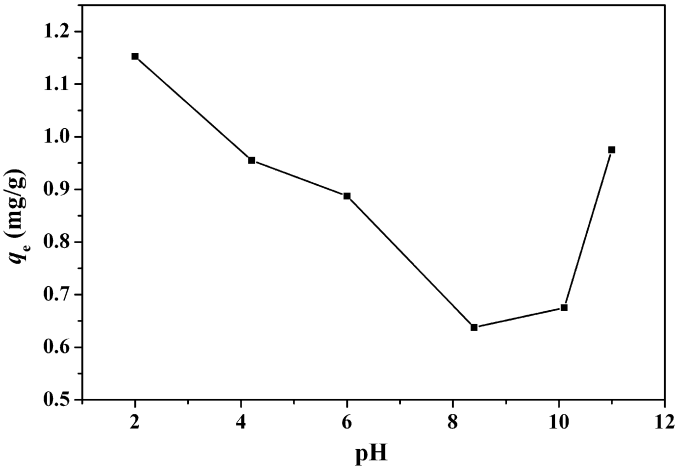

Fig. 6. Effect of pH on the phenol adsorption by HAp nanopowders at given conditions: C_0 = 10 mg/L, dosage = 4 g/L, contact time = 4 h at 20 °C, and adsorbents calcined at 120 °C.

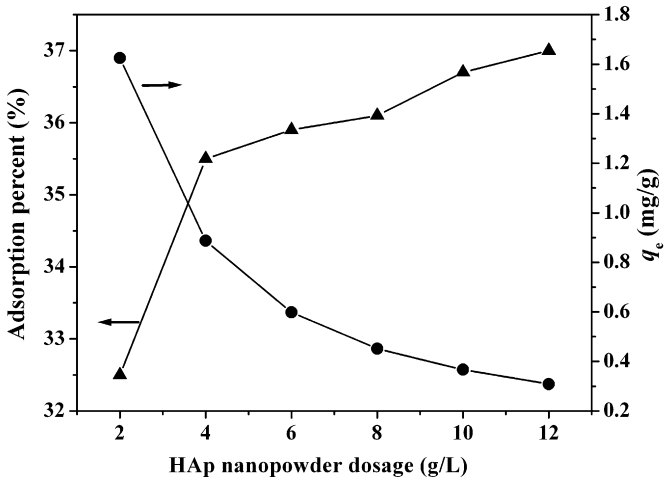

Fig. 7. Effect of HAp nanopowder dosage on phenol adsorption at given conditions: C_0 = 10 mg/L, pH 6.4, contact time = 4 h at 20 °C, and adsorbents calcined at 120 °C.

ing pH up to 8.2 and then increased with further increasing the pH to alkaline value. The maximal adsorption capacity of phenol onto HAp nanopowders was at pH 2. At low pH values, the HAp would be protonated and became positive and these led to donor–acceptor interactions between the aromatic rings of the phenol [33]. At very lower pH values, the surface of the HAp will be surrounded by the hydrogen ions, which enhance the interactions between phenol and HAp through attractive force [33]. However, at high pH values of alkalinity, the phenol would be ionized in solution and this led to increase the ionic strength [8]. The increase in the ionic strength resulted in the increase in the adsorption capacity [8]. However, the details for the effect of pH on phenol adsorption mechanism need to be further investigated.

3.4. Effect of HAp nanopowder dosage on phenol adsorption

Fig. 7 shows the adsorption percent (%) and adsorption capacity (q_e) of phenol as a function of HAp nanopowder dosage at the given conditions. It is clear to see that the increase in the HAp dosage results in an obvious increase in the phenol adsorption percent. With the increase in HAp dosage from 2 to 4 g/L, the phenol adsorption percent increased rapidly from 32.5 to 35.5%. This was because of the number of adsorption sites increased with the increase in the adsorbent dosage. With a further increase in HAp dosage to 12 g/L, the phenol adsorption percent increased slightly to 37.0%. The results also indicated that it was possible to remove phenol completely when there was sufficient HAp surface area in solution. On the other hand, the plot of adsorption capacity revealed that the adsorption capacity was high at low dosages and reduced at high dosages. Many factors can contribute to this adsorbent concentration effect. The most important factor is that adsorption sites remain unsaturated during the adsorption reaction. This is due to the fact that as the dosage of adsorbent is increased, there is less commensurate increase in adsorption resulting from the lower adsorptive capacity utilization of the adsorbent [34–36]. It is readily understood that the number of available adsorption sites increases with the increase in the adsorbent dosage and it, therefore, results in the increase in the amount of adsorbed phenol molecular. The decrease in adsorption capacity with the increase in the adsorbent dosage is mainly attributed to the unsaturation of the adsorption sites through the adsorption process [34–36]. The results of this section also indicated that, in order to obtain the optimal adsorbent dosage, higher initial phenol concentrations should be tested in conjunction with appropriate adsorbent dosage [37].

3.5. Effect of initial phenol concentration on temperature-dependent adsorption

The initial phenol concentration provides an important driving force to overcome all mass transfer limitations of phenol between the aqueous and solid phases. Therefore, a higher initial phenol concentration will enhance the adsorption process. Table 1 shows the effect of initial phenol concentration on the equilibrium adsorption capacity (q_e) and adsorption percent (%) of phenol on HAp nanopowders at different temperatures. It was clear to see that the q_e values increase with the increase in the initial phenol concentrations or the solution temperatures. The maximum equilibrium q_e values were determined as 10.18, 10.27 and 10.33 mg/g for 400 mg/L initial phenol concentrations at 20, 40 and 60 °C, respectively. However, there is no distinct difference in q_e values with the initial phenol concentration higher than 200 mg/L, which indicate that the adsorption reaches saturation at high phenol concentration because of the adsorbent offering a limited number of surface binding sites.

Al-Asheh et al. investigated the adsorption of phenol onto activated bentonites. The equilibrium uptake of phenol is 8.2–9.9 mg/g [38]. Vipulanandan determined that the phenol adsorption capacity on kaolin was 0.47 mg/g [39]. Batch adsorption of phenol on the TiO_2 nanopowders was performed by Bekkouche et al. [16] and the equilibrium phenol adsorption capacity was about 13 mg/g. The studies of Ahmaruzzaman and Sharma showed that the phenol adsorption capacity on coal was about 13 mg/g [32]. The adsorption capacity of phenol on fly ash was approximately 10 mg/g determined by Sarkar and Acharya [40]. In the present study, the adsorption capacity of phenol on HAp nanopowders was obtained as 10.18–10.33 mg/g for 400 mg/L initial phenol concentration at 20–60 °C. This result confirmed that the adsorption capacity of HAp nanopowders for phenol was similar or higher than these natural or synthetic inorganic adsorbents. However, the adsorp-

Table 1
The equilibrium uptake capacities and adsorption percent obtained at different initial concentrations and temperatures: dosage = 4 g/L, pH 6.4, contact time = 4 h, and adsorbents calcined at 120 °C

C_0 (mg/L)	20 °C		40 °C		60 °C	
	q_e (mg/g)	Adsorption percent (%)	q_e (mg/g)	Adsorption percent (%)	q_e (mg/g)	Adsorption percent (%)
2	0.29	58.00	0.31	62.40	0.35	69.40
6	0.55	36.67	0.59	39.33	0.63	41.67
10	0.89	35.60	0.89	35.60	0.91	36.40
20	1.68	33.60	1.72	34.40	1.77	35.40
30	2.24	29.87	2.30	30.67	2.36	31.47
100	6.47	25.88	6.84	27.36	7.08	28.32
200	9.93	19.86	10.22	20.44	10.26	20.52
300	9.93	13.24	10.28	13.71	10.31	13.75
400	10.18	10.18	10.27	10.27	10.33	10.33

Table 2
The equilibrium uptake capacities and adsorption percent obtained for different adsorbent calcining temperatures: C_0 = 20 mg/L, pH 6.4, dosage = 4 g/L, contact time = 4 h at the temperature of 20 °C

Samples	Adsorbent calcining temperature (°C)		
	120	600	900
q_e (mg/g)	1.68	1.57	1.18
Adsorption percent (%)	33.60	31.40	23.60

tion capacity of phenol on HAp nanopowders is low compared to the usual adsorption capacities observed with activated carbons (100–300 mg/g) [17]. This is most probably due to the small surface area of the HAp nanopowders (43.75 m^2/g) compared to those usually associated with activated carbons (around 1000 m^2/g) [17]. However, when normalized for the surface area, the adsorption capacity for the HAp nanopowders (approximately 0.23 mg/m^2) was similar to that generally observed with activated carbons (0.05–0.3 mg/m^2). However, the HAp materials possess excellent biocompatibility, easy to prepare in large scale and low-cost, which may be the merit for HAp using as adsorbent to remove the phenolic pollutants. Table 1 also demonstrates that the adsorption percent decreased with the increase in the initial phenol concentration. However, the adsorption percent showed opposite trend with the increase in the temperatures. The maximum phenol adsorption percent of the HAp nanopowders was determined as 69.40% for 2 mg/L initial phenol concentrations at 60 °C. However, the adsorption percent of the HAp nanopowders decreased to 10.33%, when the initial phenol concentration increased to 400 mg/L. The increase in the adsorption capacity and adsorption percent with the increase in the contact temperatures was due to the increase tendency of adsorbate (phenol) to adsorbent (HAp), which might also indicate that the adsorption of phenol onto the HAp nanopowders was endothermic in nature and might involve not only physical but also chemical sorption [41].

3.6. Effect of adsorbent calcining temperature on phenol adsorption

Table 2 shows the effect of HAp adsorbent calcining temperatures on phenol adsorption capacity (q_e) and adsorption percent (%). It is clear to see that the increase in the adsorbent calcining temperature result in an obvious decrease of the phenol adsorption capacity and adsorption percent on HAp nanopowders. With the increase in calcining temperature from 120 to 600 °C, the phenol adsorption capacity and adsorption percent decreased slightly from 1.68 to 1.57 mg/g, and 33.60 to 31.40%, respectively. With a further increase in the calcining temperature to 900 °C, the phenol adsorption capacity and adsorption percent decreased remarkably to 1.18 mg/g and 23.60%, respectively. The decrease of the adsorption ability was attributed to the decrease of the specific surface area (SSA) of HAp adsorbent after calcining at high temperatures. The surface properties of the adsorbents can apparently influence the adsorption properties of the organic pollutants on adsorbents. The SSA is one of the most important characteristics in the surface properties. In the inorganic material preparation process, the higher calcining temperatures can apparently decrease the SSA, which will result in the decrease of the adsorption ability. Similar results have been reported in other adsorbents for the removal of organic pollutants and heavy metal ions. The equilibrium adsorption capacity and adsorption percent of phenol increased with the increase in the SSA, suggesting that phenol adsorption onto the HAp nanopowders might be associated with surface mechanisms. Thus, surface of contact between adsorbent and the liquid phase plays an important role in the process of sorption [42]. Therefore, adsorption kinetics of phenol onto HAp was also affected by surface properties of the adsorbents.

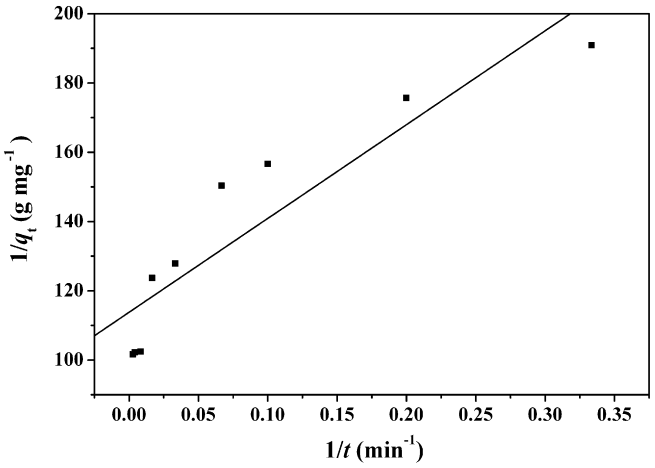

Fig. 8. The first-order kinetic model of phenol adsorption onto HAp at the temperature of 20 °C.

3.7. Kinetic modeling

Knowledge of the adsorption kinetic constitutes the first step in the investigation of the possibility of using an adsorbent for a particular separation task. In this study, the first-order kinetic model, pseudo-second-order kinetic model and an intraparticle diffusion kinetic model were used to elucidate the adsorption mechanism.

The first-order kinetic model [27] is given as:

$$\frac{1}{q_t} = \frac{k_1}{q_1}\frac{1}{t} + \frac{1}{q_1} \tag{2}$$

where q_1 and q_t are the amounts of phenol adsorbed on adsorbent at equilibrium (in mg/g) and at various time t, respectively, and k_1 is the rate constant (min^{-1}) of the first-order model for the adsorption process. Values of k_1 are calculated from the slope of the plots of $1/q_t$ versus $1/t$.

The pseudo-second-order kinetic model [28] is expressed as:

$$\frac{t}{q_t} = \frac{1}{(k_2 q_2^2)} + \frac{t}{q_2} \tag{3}$$

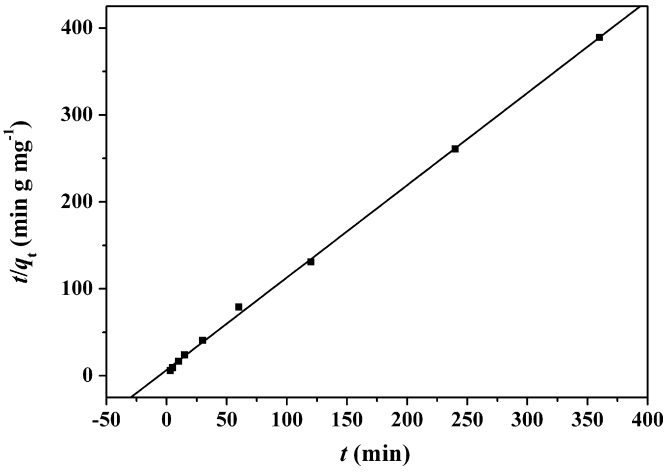

Fig. 9. The pseudo-second-order kinetic model of phenol adsorption onto HAp at the temperature of 20 °C.

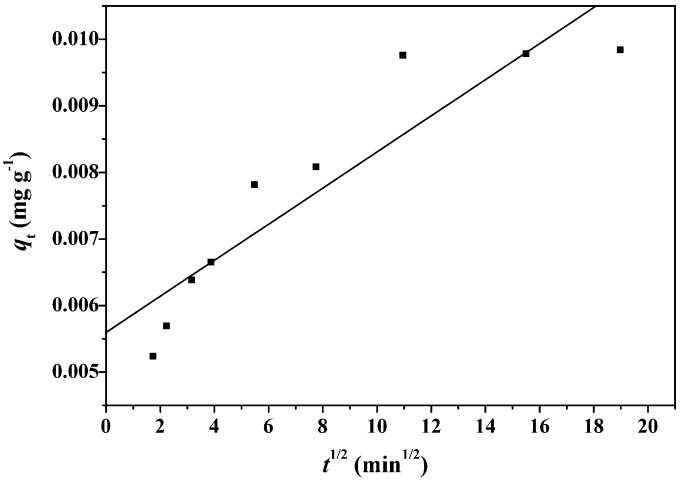

Fig. 10. The intraparticle diffusion kinetic model of phenol adsorption onto HAp at the temperature of 20 °C.

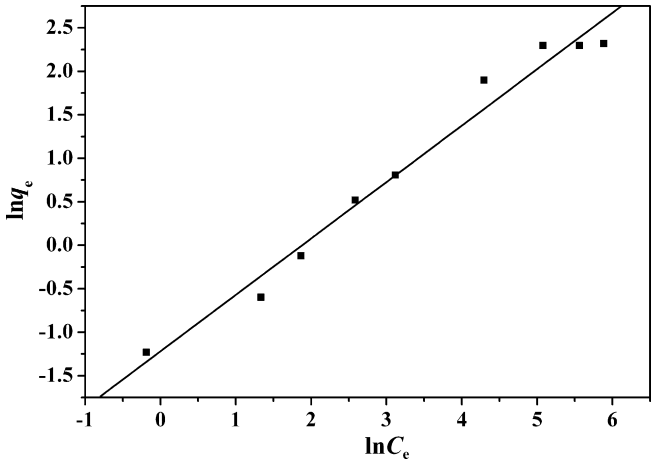

Fig. 11. The Freundlich isotherm plot for phenol adsorption onto HAp at the temperature of 20 °C.

where q_2 is the maximum adsorption capacity (mg/g) for the pseudo-second-order adsorption, q_t is the amount of phenol adsorbed at equilibrium (mg/g) at time t (min) and k_2 is the rate constant of the pseudo-second-order adsorption (g/(mg min)). Values of k_2 and q_2 were calculated from the plot of t/q_t against t.

Since neither the first-order nor the pseudo-second-order kinetic model can identify the diffusion mechanism, the intraparticle diffusion model [29] was also used to analyze and elucidate the diffusion mechanism. The intraparticle diffusion model is expressed as:

$$q_t = k_p t^{1/2} + C \tag{4}$$

where q_t is the amount of phenol adsorbed at equilibrium (mg/g) at time t, C is the intercept and k_p is the intraparticle diffusion rate constant (mg/(g min$^{1/2}$)). Values of k_p and C were calculated from the plot of q_t against $t^{1/2}$.

The straight-line plots of $1/q_t$ versus $1/t$ for the first-order model (Fig. 8), t/q_t against t for the pseudo-second-order model (Fig. 9) and the q_t versus $t^{1/2}$ for the intraparticle diffusion model (Fig. 10) of phenol adsorption onto HAp nanopowders have been tested to obtain the rate parameters at 20 °C (the plots for 40 and 60 °C were not shown). The adsorption kinetic parameters of phenol under the experimental conditions were calculated from these plots and are shown in Table 3. The correlation coefficient values (R^2) range between zero and one. A R^2 of one shows that 100% of the variation of experimental data is explained by the regression equation. The R^2 was applied to determine the relationship between the experimental data and the kinetics in most studies. The R^2, for the first-order kinetic model, pseudo-second-order kinetic model and the intraparticle diffusion kinetic model were 0.8429, 0.9992 and 0.8521, respectively. It is clear to see that the R^2 value for the pseudo-second-order kinetic model is much higher than those for the first-order kinetic and intraparticle diffusion kinetic models. Therefore, this section suggested that the pseudo-second-order model was the best choice among the three kinetic models to describe the adsorption behavior of phenol onto HAp nanopowders, suggesting that the adsorption mechanism might be a physisorption process.

3.8. Adsorption isotherms

Equilibrium data, commonly known as adsorption isotherm, is important to develop an equation that accurately represents the results and can be used in design of adsorption systems. An additional potential use of adsorption isotherms is to calculate the thermodynamic parameters. Several models have been published in the literatures to describe experimental data of adsorption equilibriums. Among them, the Langmiur [30] and Freundlich [31] models are the most frequently employed models. In this study, the Langmuir and Freundlich equilibrium isotherm models were used to describe the equilibrium between the adsorbed phenol molecular on HAp nanopowders and phenol molecular in solution at the constant temperatures. The Langmuir [30] theory is valid for monolayer adsorption onto a surface containing a finite number of identical sites, and is one of the most popular isotherm models due to its simplicity and its good agreement with experimental data. The Langmuir isotherm equation is expressed as:

$$q_e = \frac{q_m K_L C_e}{1 + K_L C_e} \tag{5}$$

where q_e is the equilibrium phenol concentration on the adsorbent (mg/g), q_m is the monolayer sorption capacity of the HAp adsorbent (mg/g) and C_e is the equilibrium phenol concentration in the solution (mg/L). The K_L is the Langmuir constant (L/mg). For fitting the experimental data, the Langmuir model was linearized as:

$$\frac{1}{q_e} = \frac{1}{q_m} + \frac{1}{q_m K_L C_e} \tag{6}$$

The Freundlich [31] isotherm model is an empirical equation and the model is valid for heterogeneous surfaces [31,43]. It assumes that the adsorption process occurs on the heterogeneous surfaces and the adsorption capacity is related to the concentration of phenol at equilibrium. The Freundlich model is generally represented as follows:

$$q_e = K_F C_e^{1/n} \tag{7}$$

Table 3
Adsorption kinitic parameters at 20 °C for different kinetic models

First-order kinetic model			Pseudo-second-order kinetic model			Intraparticle diffusion kinetic model		
k_1 (min^{-1})	q_1 (mg/g)	R^2	k_2 (g/(mg min))	q_2 (mg/g)	R^2	k_p (mg/(g min$^{1/2}$))	C (mg/g)	R^2
2.3807	0.8272	0.8429	0.1642	0.9418	0.9992	2.7×10^{-4}	0.5264	0.8521

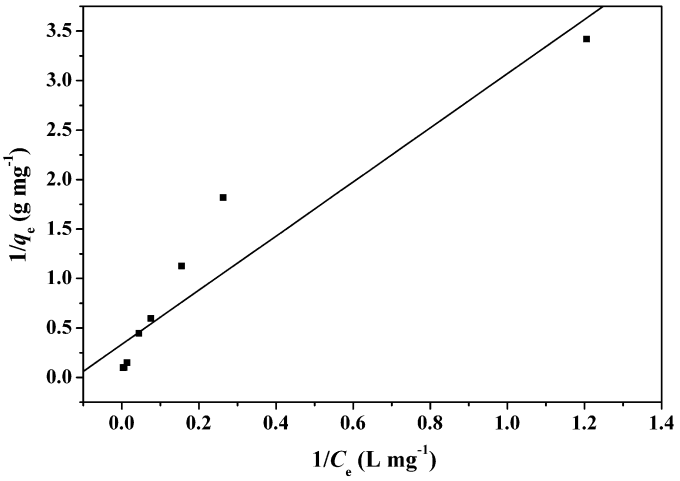

Fig. 12. The Langmuir isotherm plot for phenol adsorption onto HAp at the temperature of 20 °C.

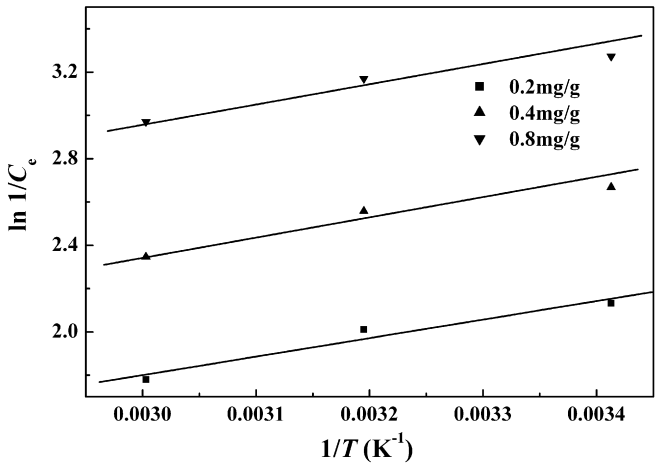

Fig. 13. Enthalpy determination curves for the adsorption of phenol onto HAp nanopowders at different adsorption capacities.

where q_e is the equilibrium phenol concentration on the adsorbent (mg/g), K_F is the empirical constant of Freundlich isotherm (L/mg) and C_e is the equilibrium concentration of the phenol in solution (mg/L). The constant n is the empirical parameter related to the intensity of adsorption, which varies with the heterogeneity of the material. When $1/n$ values are in the range $0.1 < 1/n < 1$, the adsorption process is favourable [43]. For fitting the experimental data, the Freundlich model was linearized as follows:

$$\ln q_e = \ln K_F + \frac{1}{n} \ln C_e \quad (8)$$

Figs. 11 and 12 show the fitting plots of Freundlich and Langmuir adsorption isotherms of phenol onto HAp nanopowders at 20 °C (plots at 40 and 60 °C were not shown), respectively. Table 4 summarizes the constants of the Freundlich and Langmuir isotherms obtained from the slope and intercept of the plots of each isotherm at different temperatures. Most of the R^2 values exceed 0.9 for both the Freundlich and Langmuir models, suggesting that both models closely fitted the experimental results. At the same time, the regression results demonstrated that the Freundlich isotherm fitted the experimental data better than the Langmuir isotherm. The values of K_F were 0.2954, 0.3275 and 0.3762 L/mg at 20, 40 and 60 °C, respectively. K_F increased with the increase in the temperatures, revealing that the adsorption capacity of phenol onto HAp nanopowders increased with the increase in the temperatures. Like K_F, n increased with the increase in the temperature. The highest value of n, 1.6499 at 60 °C, represents favorable adsorption at high temperature. If the n is below one, then the adsorption is chemical process; otherwise, the adsorption is physical process [44]. All values of n exceed one, suggesting the adsorption of phenol onto HAp is physical process. On the other hand, the Freundlich exponent of $1/n$ gives information about surface heterogeneity and surface affinity for the solute. The Freundlich exponent $1/n$ between 0.6061 and 0.6488 indicates favorable adsorption and a high affinity of HAp nanopowders for phenol. Gemeay [45] suggested that the higher value of $1/n$ corresponded the greater heterogeneity of the adsorbent surface. As shown in Table 4, the degree of heterogeneity of the HAp surface decreases with the increase in the temperatures.

Table 4
Isotherm parameters at various temperatures for different isotherm models

Temperature (°C)	Freundlich isotherm			Langmuir isotherm		
	K_F (L/mg)	$1/n$	R^2	q_m (mg/g)	K_L (L/mg)	R^2
20	0.2954	0.6488	0.9777	2.9841	0.1225	0.9004
40	0.3275	0.6340	0.9761	2.9324	0.1482	0.8874
60	0.3762	0.6061	0.9708	2.6954	0.2264	0.8414

With respect to the coefficients of the Langmuir model, the values of K_L were 0.1225, 0.1482 and 0.2264 L/mg at 20, 40 and 60 °C, respectively. The value of K_L increased with the increase in the temperatures, revealing that the adsorption capacity of phenol onto HAp increased with the increase in the temperature. The results also implied that the affinity of binding sites for phenol increased with the increase in the temperatures. K_L lied between zero and one, suggesting that the adsorption of phenol on HAp was favorable. Values of q_m, which is defined as the maximum capacity of adsorbents, have also been calculated from the Langmuir plots. Both the Freundlich and Langmuir models suggested that the adsorption capacity increased with the increase in the temperature, revealing that the adsorption was endothermic [46]. The following section will present the detailed thermodynamic parameters.

In summary, this section study showed that the adsorption of phenol onto the HAp nanopowders was correlated well with the Freundlich equation as compared to Langmuir equation under the concentration range studied, according to the R^2 values shown in Table 4.

3.9. Thermodynamic analyses

In any adsorption process and engineering practice, both energy and entropy factors should be considered in order to determine what processes will occur spontaneously. Values of thermodynamic parameters are the actual indicators for practical application of a process. Generally, the Gibbs free energy (ΔG°) of adsorption, enthalpy (ΔH°) and entropy (ΔS°) changes was calculated from data interpolated using the best fitting isotherm. In this study, the Freundlich isotherm was used to calculate the thermodynamic parameters using the following equations [47,48]:

$$\ln \frac{1}{C_e} = \frac{\ln K_F - \Delta H^\circ}{RT} \quad (9)$$

$$\Delta G^\circ = -nRT \quad (10)$$

$$\Delta S^\circ = \frac{\Delta H^\circ - \Delta G^\circ}{T} \quad (11)$$

where C_e is the equilibrium phenol concentration (mg/L) in the solution, n is the fitting constant of Freundlich exponent, R is the gas constant (8.314 J/(mol K)), T is the temperature (K), and K_F is the empirical constant of Freundlich. Enthalpy (ΔH°) was determined from the slope of the plots of $\ln 1/C_e$ versus $1/T$ [47,48].

Table 5
The thermodynamic parameters for adsorption of phenolic onto HAp nanpowders at various adsorption capacity and contact temperatures

Adsorption capacity (q_e, mg/g)	ΔH° (kJ/mol)	ΔG° (kJ/mol)			ΔS° (J/(mol K))		
		20 °C	40 °C	60 °C	20 °C	40 °C	60 °C
0.2	7.1115				31.1843	29.9279	28.3318
0.4	6.4756	−2.0255	−2.2559	−2.3231	29.0140	27.8962	26.4222
0.8	6.0791				27.6590	26.6295	25.2330

Fig. 13 shows the enthalpy determination curves for the adsorption of phenol onto HAp nanopowders at different adsorption capacities. Table 5 presents the thermodynamic parameters at various adsorption capacities (q_e, mg/g) and contact temperatures. The values of ΔH° were 7.1115, 6.4756 and 6.0791 kJ/mol at the adsorption capacity (q_e) of 0.2, 0.4 and 0.8 mg/g, respectively. Kara et al. [49] suggested that the ΔH° of physisorption is smaller than 40 kJ/mol. Based on ΔH°, the small positive value of the change of ΔH° (6.0791–7.1115 kJ/mol) within the range investigations in this study suggested that the adsorption of phenol onto HAp was a physisorption process in nature and was also endothermic. At the same time, the low value of ΔH° implies the loose bonding between the adsorbate molecules and the adsorbent surface [49,50]. The positive ΔS° values further suggested that the adsorption of phenol onto HAp was endothermic. Moreover, the positive ΔS° indicated that the degrees of freedom increased at the solid–liquid interface during the adsorption of phenol onto HAp. The obtained ΔG° values were −2.0255, −2.2559 and −2.3231 kJ/mol at 20, 40 and 60 °C, respectively. It is clear to see that the ΔG° values are negative at all of the tested temperatures (20–60 °C), confirming that the adsorption of phenol onto HAp is spontaneous and thermodynamically favorable. Restated, a more negative ΔG° implied a greater driving force of adsorption, resulting in a higher adsorption capacity. When the temperature increased from 20 to 60 °C, ΔG° became a higher negative value, suggesting that adsorption was more spontaneous at high temperature. Generally, the change in free energy (ΔG°) for physisorption is less than that for chemisorption. The former is between −20 and 0 kJ/mol and the latter is between −80 and −400 kJ/mol [50]. This further indicated that the physisorption might dominate the adsorption of phenol onto HAp nanopowders.

4. Conclusions

In this study, the adsorption potential of HAp nanopowders was investigated for the removal of phenol from aqueous solutions. The effect of contact time, initial phenol concentration, pH, adsorbent dosage, phenol solution temperature and adsorbent calcining temperature on the phenol adsorption by HAp nanopowders was determined. The kinetic, equilibrium and thermodynamic of the adsorption of phenol onto HAp nanopowders was investigated with variations in phenol concentration and contact time at various temperatures. The following results were obtained:

- The nano-size HAp powders were prepared by the chemical precipitation method. The preparation procedures had showed that increase in the calcining temperature could obvious decrease the specific surface area (SSA) of the HAp nanopowders. The decrease of the SSA of the adsorbents resulted in the decrease of the adsorption capacity and adsorption percent for the phenol.
- The adsorption process was very fast, and it reached equilibrium in 2 h of contact, which is much faster than that of some other normal adsorbents for the removal of phenol.
- The pH and the adsorbent calcining temperature played an obvious effect on the phenol adsorption capacity onto HAp nanopowders. Increase in the pH to high-acidity or to high-alkalinity resulted in the increase in the phenol adsorption capacity.
- Increase in the initial phenol concentration and contact temperature could increase the phenol adsorption capacity. However, the higher HAp dosage led to the decrease of the phenol adsorption capacity.
- The kinetic data fitting results showed that the adsorption of phenol onto HAp nanopowders followed the pseudo-second-order kinetic model.
- The equilibrium adsorption isotherm of phenol onto HAp was well described by Langmuir and Freundlich model, but the Freundlich model fitted the experimental data better than Langmuir model.
- Thermodynamic calculations showed that the phenol adsorption process by HAp was physisorption, spontaneous and endothermic in nature. Increase in the contact temperature resulted in the increase in the phenol adsorption capacity.
- The enthalpy change (ΔH°) for the adsorption process has small values (6.0791–7.1115 kJ/mol) indicating the loose bonding between the adsorbate molecules (phenol) and the adsorbent (HAp) surface.
- The results showed that the HAp nanopowders might be a new potential, biocompatible and good adsorbent for the removal of phenol pollutants from aqueous solutions.

Acknowledgement

This work was supported by grants from Science and Technology Commission of Shanghai Municipality (Grant No. 05nm05042).

Appendix A

$$q_e = (C_0 - C_t)\frac{V}{m} \quad (A.1)$$

$$\frac{1}{q_t} = \frac{k_1}{q_1}\frac{1}{t} + \frac{1}{q_1} \quad (A.2)$$

$$\frac{t}{q_t} = \frac{1}{(k_2 q_2^2)} + \frac{t}{q_2} \quad (A.3)$$

$$q_t = k_p t^{1/2} + C \quad (A.4)$$

$$q_e = \frac{q_m K_L C_e}{1 + K_L C_e} \quad (A.5)$$

$$\frac{1}{q_e} = \frac{1}{q_m} + \frac{1}{q_m K_L C_e} \quad (A.6)$$

$$q_e = K_F C_e^{1/n} \quad (A.7)$$

$$\ln q_e = \ln K_F + \frac{1}{n}\ln C_e \quad (A.8)$$

$$\ln\frac{1}{C_e} = \frac{\ln K_F - \Delta H^\circ}{RT} \quad (A.9)$$

$$\Delta G^\circ = -nRT \quad (A.10)$$

$$\Delta S^\circ = \frac{\Delta H^\circ - \Delta G^\circ}{T} \quad (A.11)$$

References

[1] S. Rengaraj, S.H. Moon, R. Sivabalan, B. Arabindoo, V. Murugesan, Removal of phenol from aqueous solution and resin manufacturing industry wastewater using an agricultural waste: rubber seed coat, J. Hazard. Mater. 89 (2002) 185–196.

[2] S. Rengaraj, S.H. Moon, R. Sivabalan, B. Arabindoo, V. Murugesan, Agricultural solid waste for the removal of organics: adsorption of phenol from water and wastewater by palm seed coat activated carbon, Waste Manage. 22 (2002) 543–548.

[3] N. Roostaei, F.H. Tezel, Removal of phenol from aqueous solutions by adsorption, J. Environ. Manage. 70 (2004) 157–164.

[4] M. Akcay, Characterization and determination of the thermodynamic and kinetic properties of p-cp adsorption onto organophilic bentonite from aqueous solution, J. Colloid Interface Sci. 280 (2004) 299–304.

[5] O.J. Hao, H. Kim, P.C. Chiang, Decolorization of wastewater, Crit. Rev. Environ. Sci. Technol. 30 (2000) 449–505.

[6] B. Özkaya, Adsorption and desorption of phenol on activated carbon and a comparison of isotherm models, J. Hazard. Mater. 129 (2006) 158–163.

[7] J.H. Tay, X.G. Chen, S. Jeyaseelan, N. Graham, Optimising the preparation of activated carbon from digested sewage sludge and coconut husk, Chemosphere 44 (2001) 45–51.

[8] A. Dabrowski, P. Podkoscielny, M. Hubicki, M. Barczak, Adsorption of phenolic compounds by activated carbon—a critical review, Chemosphere 58 (2005) 1049–1070.

[9] S.K. Dentel, I.Y. Bottero, K. Khatýb, H. Demovgeot, I.P. Duguet, C. Anselme, Sorption of tannic acid, phenol and 2,4,5-trichlorophenol on organoclays, Water Res. 29 (1995) 1273–1280.

[10] F.C. Wu, R.L. Tseng, R.S. Juang, Adsorption of dyes and phenols from water on the activated carbons prepared from corncob wastes, Environ. Technol. 22 (2001) 205–213.

[11] S.H. Lin, M.J. Cheng, Adsorption of phenol and *m*-chlorophenol on organobentonites and repeated thermal regeneration, Waste Manage. 22 (2002) 595–603.

[12] X. Zhang, A.M. Li, Z.M. Jiang, Q.X. Zhang, Adsorption of dyes and phenol from water on resin adsorbents: effect of adsorbate size and pore size distribution, J. Hazard. Mater. 137 (2006) 1115–1122.

[13] N. Yildiz, H. Kapucu, A. Calimli, Response surface optimization of the phenol adsorption on to HDTMA-bentonite, Rev. Chem. Eng. 16 (2000) 55–70.

[14] B. Koumanova, P.P. Antova, Adsorption of *p*-chlorophenol from aqueous solutions on bentonite and perlite, J. Hazard. Mater. A90 (2002) 229–234.

[15] M.A. Ulibarri, I. Pavlovic, M.C. Hermosin, J. Cornejo, Hydrotalcite-like compounds as potential sorbents of phenols from water, Appl. Clay Sci. 10 (1995) 131–145.

[16] S. Bekkouche, M. Bouhelassa, N. Hadj Salah, F.Z. Meghlaoui, Study of adsorption of phenol on titanium oxide (TiO_2), Desalination 166 (2004) 355–362.

[17] H. Polat, M. Molva, M. Polat, Capacity and mechanism of phenol adsorption on lignite, Int. J. Miner. Process. 79 (2006) 264–273.

[18] S. Richards, A. Bouazza, Phenol adsorption in organo-modified basaltic clay and bentonite, Appl. Clay Sci. 37 (2007) 133–142.

[19] J.Q. Jing, C. Cooper, S. Ouki, Comparison of modified montmorillonite adsorbents. Part I. Preparation, characterization and phenol adsorption, Chemosphere 47 (2002) 711–716.

[20] A. Slosarczyk, J.S. Oleksiak, B. Mycek, The kinetics of pentoxifylline release from drug-loaded hydroxyapatite implants, Biomaterials 21 (2000) 1215–1221.

[21] R.M. Schek, E.N. Wilke, S.J. Hollister, P.H. Krebsbach, Combined use of designed scaffolds and adenoviral gene therapy for skeletal tissue engineering, Biomaterials 27 (2006) 1160–1166.

[22] A. Tiselius, S. Hjerten, O. Levin, Protein chromatography on calcium phophate columns, Arch. Biochem. Biophys. 65 (1965) 132–155.

[23] O. Takagi, N. Kuramoto, M. Ozawa, S. Suzuki, Adsorption/desorption of acidic and basic proteins on needle-like hydroxyapatite filter prepared by slip casting, Ceram. Int. 30 (2004) 139–143.

[24] J.G. Del Rio, P. Sanchez, P.J. Morando, D.S. Cicerone, Retentionion of Cd, Zn and Co on hydroxyapatite filters, Chemosphere 64 (2006) 1015–1020.

[25] B. Sandrine, N. Ange, B.A. Didier, C. Eric, S. Patrick, Removal of aqueous lead ions by hydroxyapatites: equilibria and kinetic processes, J. Hazard. Mater. 139 (2007) 443–446.

[26] Q.M. Wei, T. Nakato, Competitive adsorption of phenols on organically modified layered hexaniobate $K_4Nb_6O_{17}$, Microporous Mesoporous Mater. 26 (2006) 84–92.

[27] N. Kannan, M.M. Sundaram, Kinetics and mechanism of removal of methylene blue by adsorption on various carbons-a comparative study, Dyes Pigments 51 (2001) 25–40.

[28] Y.S. Ho, G. McKay, Sorption of dye from aqueous solution by peat, Chem. Eng. J. 70 (1998) 115–124.

[29] W.J. Weber Jr., J.C. Morriss, Kinetics of adsorption on carbon from solution, J. Sanit. Eng. Div. Am. Soc. Civ. Eng. 89 (1963) 31–60.

[30] I. Langmuir, The adsorption of gasses on plane surface of glass, mica and platinum, J. Am. Chem. Soc. 40 (1916) 1361–1368.

[31] H.M.F. Freundlich, Über die adsorption in lösungen, Z. Phys. Chem. 57 (1906) 385–470.

[32] M. Ahmaruzzaman, D.K. Sharma, Adsorption of phenols from wastewater, J. Colloid Interface Sci. 287 (2005) 14–24.

[33] X.L. Chai, Y.C. Zhao, Adsorption of phenolic compound by aged-refuse, J. Hazard. Mater. 137 (2006) 410–417.

[34] R.P. Han, W.H. Zou, Z.P. Zhang, J. Shi, J.J. Yang, Removal of copper(II) and lead(II) from aqueous solution by manganese oxide coated sand. I. Characterization and kinetic study, J. Hazard. Mater. 137 (2006) 384–395.

[35] Y.S. Ho, C.C. Chiang, Sorption studies of acid dye by mixed sorbents, Adsorption 7 (2001) 139–147.

[36] Y.C. Hsu, C.C. Chiang, M.F. Yu, Adsorption behaviors of basic dyes on activated clay, Sep. Sci. Technol. 32 (1997) 2513–2534.

[37] Y.S. Ho, C.C. Chiang, Y.C. Hsu, Sorption kinetics for dye removal from aqueous solution using activated clay, Sep. Sci. Technol. 36 (2001) 2473–2488.

[38] S. Al-Asheh, F. Banat, L. Abu-Aitah, Adsorption of phenol using different types of activated bentonites, Sep. Purif. Technol. 33 (2003) 1–10.

[39] C. Vipulanandan, Effect of clays and cement on the solidification/stabilization of phenol-contaminated soils, Waste Manage. 15 (1995) 399–406.

[40] M. Sarkar, P.K. Acharya, Use of fly ash for the removal of phenol and its analogues from contaminated water, Waste Manage. 26 (2006) 559–570.

[41] G. Dursun, H. Cicek, A.Y. Dursun, Adsorption of phenol from aqueous solution by using carbonized beet pulp, J. Hazard. Mater. 125 (2005) 175–182.

[42] J. Wu, H.Q. Yu, Biosorption of 2,4-dichlorophenol from aqueous solution by *Phanerochaete chrysosporium* biomass: Isotherms, kinetics and thermodynamics, J. Hazard. Mater. 137 (2006) 498–508.

[43] I. Vázquez, J. Rodríguez-Iglesias, E. Marañón, L. Castrillón, M. Álvarez, Removal of residual phenols from coke wastewater by adsorption, J. Hazard. Mater., in press.

[44] J.Q. Jiang, C. Cooper, S. Ouki, Comparison of modified montmorillonite adsorbents. Part I. Preparation, characterization and phenol adsorption, Chemosphere 47 (2002) 711–716.

[45] A.H. Gemeay, Adsorption characteristics and the kinetics of the cation exchange of rhodamine-6G with Na^+-montmorillonite, J. Colloid Interface Sci. 251 (2002) 235–241.

[46] C.H. Wu, Adsorption of reactive dye onto carbon nanotubes: equilibrium, kinetics and thermodynamics, J. Hazard. Mater. 144 (2007) 93–100.

[47] R.A. Garcia-Delgado, L.M. Cotouelo-Minguez, J.J. Rodriguez, Equilibrium study of single-solution adsorption of anionic surfactants with polymeric XAD resins, Sep. Sci. Technol. 27 (1992) 975–987.

[48] J.P. Bell, M. Tsezos, Removal of hazardous organic pollutions by biomass adsorption, J. Water Pollut. Control. Fed. 59 (4) (1987) 191–198.

[49] M. Kara, H. Yuzer, E. Sabah, M.S. Celik, Adsorption of cobalt from aqueous solutions onto sepiolite, Water Res. 37 (2003) 224–232.

[50] M.J. Jaycock, G.D. Parfitt, Chemistry of Interfaces, Ellis Horwood, Chichester, 1981.